Enhancing $CuIn_{0.7}Ga_{0.3}Se_2$ Solar Cells: The Role of Alkali Treatment in Single-Stage Co-Evaporation

Elijah Young[1], Grace Young[1], Mia Roberts[2]

[1] Institute for Material Research (IMO), Hasselt University (partner in Solliance & EnergyVille), Agoralaan gebouw H, Diepenbeek, 3590, Belgium
[2] Imec division IMOMEC (partner in Solliance & EnergyVille), Wetenschapspark 1, 3590 Diepenbeek, Belgium.
[3] TNO Solliance, High Tech Campus 21, 5656 AE Eindhoven, The Netherlands
[4] imec (partner in Solliance & EnergyVille), Kapeldreef 75, Leuven, 3001, Belgium
[5] Department of Electrical Engineering, KU Leuven, Kasteelpark Arenberg 10, 3001 Heverlee, Belgium

Abstract

KF and NaF treatments were done for single-stage co-evaporated $CuIn_{0.7}Ga_{0.3}Se_2$. The absorber layers were grown on a substrate with an alkali barrier layer and NaF was either added before or after absorber layer growth. No differences were found on the device performance amongst the procedures to add Na. This is expected if the single-stage process does not have a copper rich stage or a Ga gradient, which is likely since there was no change of the elemental fluxes during absorber layer growth and no Ga profile was measured. KF was added by post-deposition only. Current-voltage characteristics were measured and net doping concentrations were determined from capacitance-voltage measurements (CV). We see an improvement of the open-circuit voltage (V_{oc}) with increasing KF amount, and a marginal increase of the fill factor. CV measurements showed increasing net acceptor concentration with increasing KF amount. Time resolved photoluminescence (PL) showed an increased decay time for KF treated cells and the PL peak shape changed. Without KF treatment the PL peak is symmetric, after KF treatment a further peak appears at higher energy in the PL spectrum. This higher energy peak increases in intensity with increasing KF concentration. The same effects were seen in a sample without Na, but here the V_{oc} was limited due to large tailing. Hence both Na and K are required for good cell efficiencies.

1. Introduction

Thin film $CuIn_{0.7}Ga_{0.3}Se_2$ (CIGS) solar cells have reached efficiencies close to 23% [1] by using several alkali treatments. Despite these high laboratory efficiencies CIGS is still lagging on module efficiencies, mainly due to the complex 3-stage co-evaporation process required to reach these high efficiencies. The 3-stage co-evaporation process is an advanced process that involves a copper rich stage and a Ga gradient. While this leads to high efficiency cells it also makes the process complex, more difficult to upscale and increases the cost of CIGS modules due to the high amount of material required. There are several ways to improve the cost performance, like increasing the efficiency and/or reducing processing costs. We aim to make CIGS thinner (~ 500 nm) and to use a single-stage process to make CIGS more cost effective. The single-stage co-evaporation process increases the production speed, while thinner cells lead to less material usage and thereby reduces the absolute amount of alkali metals. While alkali metals are required to reach high efficiencies, they cause degradation on the long term due to diffusion towards the interfaces [2,3] and hence the amount needs to be carefully controlled. Here we investigate the effect of Na and K on the performance of thin single-stage CIGS solar cells.

The effect of Na is broad and widely investigated. It is known to increase the net acceptor concentration [4,5], it affects the crystal size during growth [6] and the diffusion of Ga towards the back contact [7]. The latter two effects are attributed to a copper rich phase during growth and the presence of a Ga gradient. In these cases, it also matters whether the Na supply is realized by post or pre-deposition. The effects of the KF post-deposition treatment (PDT) are still under discussion, but it also increases the net acceptor concentration [8]. However, it mostly seems to modify the CIGS/CdS interface positively [9–11]. Here, KF treatment is performed by post-deposition treatment only.

For our single-stage samples we investigated the effect of the different alkali treatments on the device performance. At first, we investigate the effect of Na

addition before and after absorber layer growth. There were no significant differences between the different Na treatments on the electrical performance of solar cells found. A reference sample without any Na was made and we indeed see an increase in net acceptor concentration with Na compared to the sample w/o Na. Based on the Na experiments, we spin-coated one layer of NaF before CIGS growth, since this eliminated a separate PDT step. The KF treatments were done post-deposition and samples with only Na were used as reference. With the KF treatment large improvements were found for the open-circuit voltage (V_{oc}), the net acceptor concentration and the decay time. The photoluminescence (PL) spectra revealed an additional peak at higher energy.

2. Experimental details

CIGS layers are deposited at 550 °C on Mo/Si(O,N)/soda lime glass substrates. The Si(O,N) layer is ~ 140 nm and functions as an alkali barrier layer. That way, the alkali concentrations are controlled by pre- and post-deposition treatments only. The CIGS layers are deposited by single-stage co-evaporation. The crucible temperatures are set in such a way that the evaporation rate of each element to the substrate immediately leads to the required composition. When the evaporation rates are stabilized the shutter is opened for 7.30 minutes, which results in a thickness of about 0.5 μm. Exact composition and thickness were measured with XRF. No gradients in elemental concentration profiles were measured by GDOES (not shown). This is in contrast to other single-stage processes, where Ga profiles were added on purpose by changing the evaporation rates to the substrate [12]. Na was added by dissolving NaF in deionized water and spin-coating a 0.2 M NaF solution with a speed of 3000 rpm and acceleration of 5000 rpm/s for 10 s in total. This was either done on a Mo substrate or after CIGS deposition. KF treatments were always done after the growth of the CIGS absorber layers using the same spin-coating process as for NaF. The post-deposition samples were annealed in a N_2 atmosphere for 20 minutes at 400 °C.

To avoid degradation of the surface, the CIGS absorber layers were directly capped with CdS by chemical bath deposition. Solar cells were prepared by sputtering i-ZnO/Al:ZnO window layers and finished with Ni/Al grids. PL and time-resolved PL (TRPL) were measured with a fluorescence spectrometer from Hamamatsu at room temperature. As excitation source a 15 kHz laser with a wavelength of 532 nm was used. The power was 1 mW and the spot size ~ 30 mm^2. The solar cells were characterized by a homebuilt current-voltage (JV) and capacitance-voltage (CV) set up. The frequency varied from 1 kHz to 1 MHz. External quantum efficiency (EQE) measurements were performed with a Bentham PVE300 photovoltaic QE system. The resolution was set to 10 nm and band gaps were determined from tauc plots.

3.Results

3.1NaF treatment of single-stage co-evaporated $CuIn_{0.7}Ga_{0.3}Se_2$

Absorber layers were prepared with a Cu/(In + Ga) ratio (GGI) of 0.8 and Ga/(Ga + In) ratio (CGI) of 0.27. The thickness varied from 0.39 to 0.49 μm. The absorber layers underwent different NaF treatments and were directly finished into solar cells. The different Na treatments (thickness) were as follows: without (w/o) Na (0.49 μm), pre-NaF deposition 1 layer (0.39 μm), post-NaF deposition 1 layer (0.49 μm), post-NaF deposition 2 layers (0.49 μm) and pre-NaF deposition 1 layer but undergoing the post treatment anneal without NaF deposition (0.47 μm). The latter one is for reference of the post treatment anneal itself. The solar cells have an area of 0.5 cm^2 and were mechanically scribed. The number of cells that are measured varied between 5 to 7 on 5x5 cm^2 samples. The results of the JV measurements are presented in Figure 1. We find no significant differences in V_{oc} and fill factor (FF) between the different Na treatments. The differences in short circuit current density (J_{sc}) can directly be attributed to the different absorber layer thicknesses. The findings are in contrast with the 3-stage process where post-deposition treatment is preferred. This is likely due to the lack of a

copper rich phase and corresponding grain growth during the deposition process. Also, increasing the amount of Na by PDT does not affect the final performance significantly. The only sample showing significant different V_{oc}, J_{sc} and FF is the one without any Na treatment. It has a lower V_{oc} and FF but higher J_{sc}. This can be attributed to lower apparent doping concentration. Doping profiles were determined from CV measurements at different frequencies and the results are presented in Figure 2. We find a 3 times lower doping for the cells without Na, compared to the solar cell that has 1 layer NaF PDT. The doping profile of this latter solar cell is representative for all Na treated solar cells. The effect of the post anneal itself is also shown in figure 1 under the name 'pre + post anneal'. We again find no significant differences and we conclude that the anneal treatment itself does not influence the solar cell properties significantly.

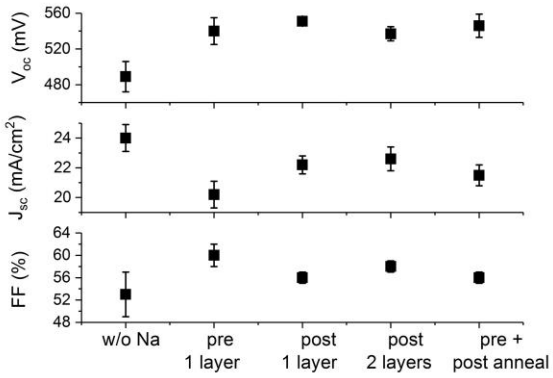

Figure 1 Average values of V_{oc}, J_{sc} and FF for different Na treatments. No significant difference between the different Na treatments is observed. The cells without Na gave a lower V_{oc} and FF and higher J_{sc} which is caused by the lower net doping.

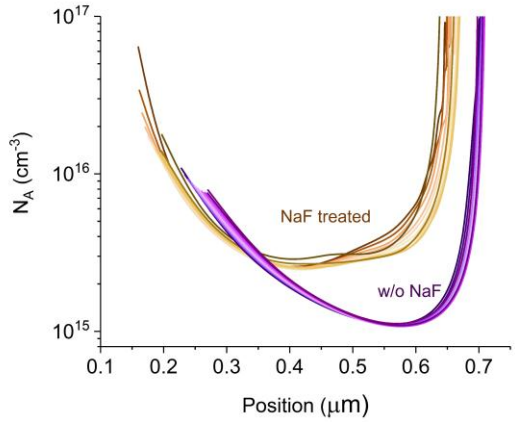

Figure 2 Net doping (N_A) extracted from capacitance-voltage measurements of absorbers with 1 layer NaF PDT and without NaF. The different shades of color represent the different frequencies.

3.2KF post deposition treatment

KF post deposition treatments were done by spin-coating 0.1 M and 0.2 M KF solutions on CIGS absorbers followed by annealing the samples at 400 °C for 20 min in N_2 atmosphere. Spinning parameters are the same as those used for NaF. The Na was added by pre-deposition. As reference a sample without KF was annealed as well and further processed in the same way as the KF treated cells. The CGI of the samples was between 0.86 - 0.9 and the GGI was 0.3. The thickness was 0.47 μm for the samples w/o KF and 0.1 M KF and 0.43 μm for the samples 0.2 M KF and 0.2 M KF w/o NaF. In figure 3 average values for V_{oc}, J_{sc} and FF are presented. We see a significant increase of the V_{oc} from ~ 550 mV to 610 mV for the 0.2 M KF treated cells. The 0.1 M KF treated cells only show a marginal increase. The FF is on average slightly higher for the KF treated cells as well. At last KF treatment (0.2 M) was done on an absorber without any Na pre-treatment. Here, the V_{oc} is slightly higher than for the cells without KF (and only Na pre-treatment) and the FF the highest. The same trend was observed when comparing pure NaF PDT with pure KF PDT [10]. The J_{sc} varied between 20 and 22 mA/cm^2. The lower and higher values are corresponding with the

different thicknesses of the absorber layers. From EQE measurements band gaps between 1.18 and 1.20 eV were determined (not shown here), thus the V_{oc} improvements can be attributed to the alkali treatments and are not caused by variations in the Ga content. In table 1, values for the highest V_{oc}, corresponding FF and doping determined from CV measurements are given. Doping profiles of the KF treated samples and the reference are presented in figure 4. The KF treated cells without Na pre-treatment had the same profile as the 0.2 M KF treated cells with Na pre-treatment but were left out for clarity of the figure. This implies that the doping is determined by the KF treatment. When we look at the different doping profiles, we observe significant differences between the KF treated and non-KF-treated samples. Firstly, the acceptor concentration is increasing with increasing KF amount. This by itself could lead to the observed V_{oc} improvement, like we measured for Na/no Na cells. However, the cells without Na have a significant lower V_{oc}, but the same doping level. This excludes V_{oc} improvements due to increase in doping only. Secondly, we find that the doping profile is dependent on the frequency for the KF treated cells. The frequency dependence of the capacitance of thin film solar cells is widely explored and has led to a variety of explanations. At first, the different frequencies may probe different defects within the band gap, which results in an increased capacitance. The observed shift is then interpreted as a newly formed defect due to the KF PDT. More recently though, the frequency dependent CV measurements of alkali treated CIGS are interpreted as a transport barrier at the front [13] or deep defects at the pn junction [14]. To conclude on what causes the measured shift with the KF treatment, more advanced characterization like low temperature CV and JV measurements are required.

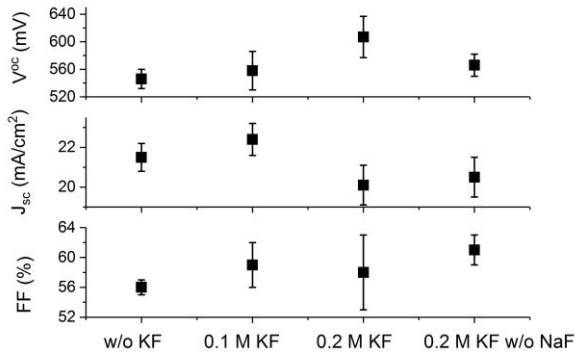

Figure 3 Average values of V_{oc}, J_{sc} and FF for different KF treatments. Na was supplied by pre-treatment.

Table 1 Parameters of the best cells for the different KF treatments shown in figure 3.

Na supply	K supply	Highest V_{oc} (mV)	Highest FF (%)	Doping (10^{16} cm^3)
pre	w/o	564	57	0.2
pre	0.1 M	590	62	0.3-0.5
pre	0.2 M	641	64	0.4-0.7
w/o	0.2 M	586	64	0.4-0.7

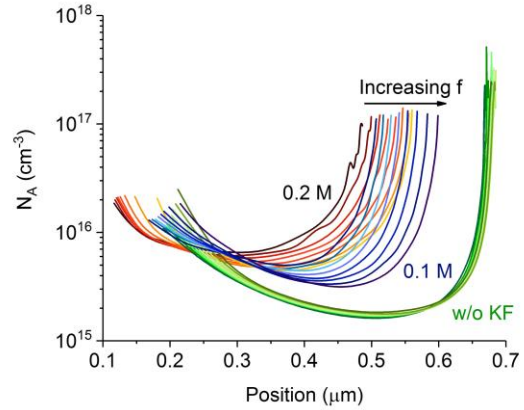

Figure 4 Net doping extracted from capacitance-voltage measurements at different frequencies for absorbers with(out) KF treatment. After KF treatment the net acceptor doping has increased and the cells have depletion width dependency on the frequency.

3.3Photoluminescence

Room temperature PL and TRPL were done on absorber layers capped with CdS and finished solar cells. At room temperature the PL peak maximum is expected just above the bandgap energy [15]. However, in disordered semiconductors significant emission can also come from the tail states. Figure 5 shows the PL spectra of the absorber layers capped with CdS with and w/o Na after 0.2 M KF treatment. The measurement conditions were the same. The individual spectra are fitted with 2 Gaussian shaped peaks and the values of the fit are given in table 2. Both spectra are shown in the upper graph for comparison. As we can see, there is a significant amount of emission below the band gap of ~ 1.2 eV (red peak), probably coming from tail states. That our absorbers have large amount of tails can be attributed to the small grain size and the presence of extended defects due to the single-stage process [16]. The high energy peak (green peak) is likely coming from the band edge. A few differences between the two samples can be observed. At first, we find that the low energy peak of the sample without Na is broader than that of the sample with Na. Secondly, we observe that the emission intensity is lower for the sample w/o Na as well. This broadened low energy peak and lower intensity should reduce the V_{oc}. These absorber layers were further processed into the solar cells belonging to 0.2 M KF and 0.2 M KF w/o NaF and indeed a lower V_{oc} (~ 40 mV) was measured for the sample w/o NaF. The PL spectra of finished solar cells w/o KF, 0.1 M KF and 0.2 M KF with Na pre-treatment are presented in figure 6. There is a marginal difference in peak intensity for the solar cells (up to 1.2 times) and we show the normalized spectra. The spectra are fitted with Gaussian shaped peak profiles and the peak maxima are given in table 2. We clearly see again two distinguishable peaks for the KF treated cells, while for the sample w/o KF the spectra can be fitted with one broad distribution. It seems that the band edge emission for the sample w/o KF is indistinguishable from the tail emission. After KF treatment the tail emission

might be reduced, leading to the observed disentanglement of the band edge and tail states emission peaks.

Table 2 Peak maxima extracted from fit of PL spectra shown in figure 6 with Gaussian shaped peaks.

Sample	Low energy peak (eV)	FWHM (meV)	High energy peak (eV)	FWHM (meV)
0.2 M KF w NaF CIGS/CdS	1.11	73	1.20	104
0.2 M KF w/o NaF CIGS/CdS	1.10	125	1.21	80
w/o KF w NaF Solar cell	1.17	103	-	-
0.1 M KF w NaF Solar cell	1.16	82	1.22	77
0.2 M KF w NaF Solar cell	1.15	86	1.23	81

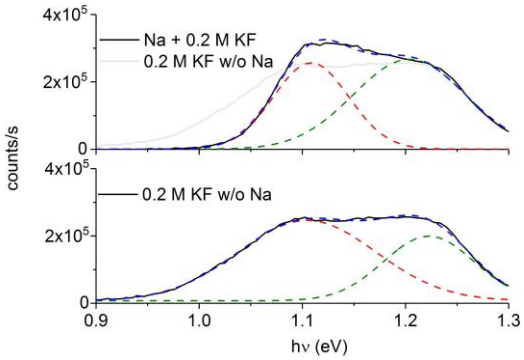

Figure 5 Photoluminescence spectra of absorber layers that underwent KF PDT with (upper graph) and without (lower graph) Na pre-treatment. The spectra are fitted with two Gaussian shaped peaks. For intensity and shape comparison, both spectra are plotted in the upper graph. The sample without Na has a lower intensity and a broader tail (red peak).

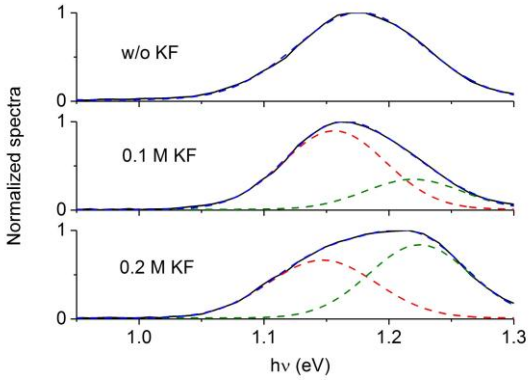

Figure 6 Room temperature photoluminescence spectra of finished solar cells. The spectra are fitted with Gaussian shaped peaks. Without KF treatment the PL spectra can be fitted with one broad Gaussian.

TRPL transients of the solar cells are shown in figure 7. Decay times significantly increase with the explored KF treatments. However, there is no relationship with the total amount of KF. Decay time is the inverse of the sum of several concurrent recombination or charge extraction processes and depends on the presence of an electric field. Though, the latter is beyond the detection limit of the set up. Hence, improvements are observed if the limiting decay time is increased or if there are no charge extraction processes. Since we don't expect significant changes for the charge extraction processes, we attribute the increase in lifetime to reduced recombination. At this stage it is hard to say whether the increase is due to reduced recombination in the bulk or at the interface. From literature we know that the CdS/CIGS interface improves with KF treatment and that the alkali metals accumulate at the pn junction and back contact [10,11]. This will change recombination rates at the interfaces which will affect the decay time for thin layers like ours. However, we also find changes in the bulk as we can conclude from the PL spectra and the doping profile. Hence, it is likely a combined effect and more experiments on both finished devices and the absorber layers are required to differentiate.

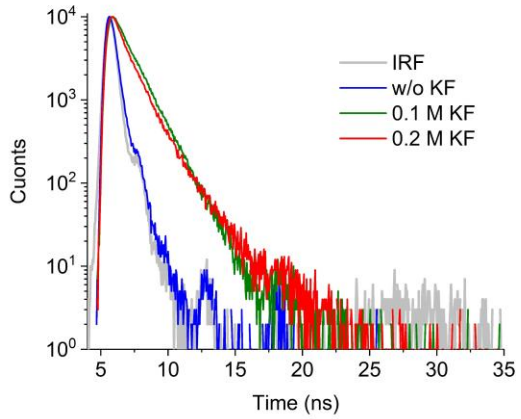

Figure 7 Room temperature time resolved photoluminescence of finished solar cells. The KF treated cells show a clear increase of decay time. The light grey curve is the instrumental response function (IRF).

4. Conclusion

We have investigated the effects of NaF and KF treatments on thin single-stage CIGS absorbers, either performed by pre-deposition or post-deposition treatment in N_2 atmosphere. We found that for the device performance it did not matter whether Na was added before or after absorber layer growth. This was attributed to the constant elemental flux during CIGS growth that leads to the absence of a copper rich stage and a Ga gradient. KF treatment was done by post-deposition only and we found significant improvements in device performance for higher concentrations of KF. All KF treated cells showed similar changes in CV measurements, PL spectra and TRPL transients. The PL spectra revealed a second peak at higher energy and the TRPL an increased decay time. From CV measurement a higher net acceptor concentration was determined. One sample without Na underwent only KF treatment. It revealed the same features in the PL spectra and doping profile as the other KF treated samples, but the solar cells had a lower V_{oc} compared to the sample that had Na. The PL spectra revealed a broader tail for this sample, which likely limited the V_{oc}. It shows that both alkali metals are required to obtain good cell efficiencies.

Acknowledgements

This work received funding from the European Union's H2020 research and innovation program under grant agreement No. 715027

References

[1] P. Jackson, R. Wuerz, D. Hariskos, E. Lotter, W. Witte, M. Powalla, Effects of heavy alkali elements in Cu(In,Ga)Se $_2$ solar cells with efficiencies up to 22.6%, Phys. Status Solidi - Rapid Res. Lett. 10 (2016) 583–586. doi:10.1002/pssr.201600199.

[2] M. Theelen, V. Hans, N. Barreau, H. Steijvers, Z. Vroon, M. Zeman, The impact of alkali elements on the degradation of CIGS solar cells, Prog. Photovoltaics Res. Appl. 23 (2015) 537–545. doi:10.1002/pip.2610.

[3] B. Vermang, F. Rostvall, V. Fjällström, M. Edoff, Potential-induced optimization of ultra-thin rear surface passivated CIGS solar cells, Phys. Status Solidi - Rapid Res. Lett. 8 (2014) 908–911. doi:10.1002/pssr.201409387.

[4] D.J. Schroeder, A.A. Rockett, Electronic effects of sodium in epitaxial CuIn1−xGaxSe2, J. Appl. Phys. 82 (1998) 4982. doi:10.1063/1.366365.

[5] T. Nakada, D. Iga, H. Ohbo, A. Kunioka, Effects of Sodium on $\boldsymbol{Cu(In,Ga)Se_2}$ -Based Thin Films and Solar Cells, Jpn. J. Appl. Phys. 36 (1997) 732–737. doi:10.1143/JJAP.36.732.

[6] H. Stange, S. Brunken, H. Hempel, H. Rodriguez-Alvarez, N. Schäfer, D. Greiner, A. Scheu, J. Lauche, C.A. Kaufmann, T. Unold, D. Abou-Ras, R. Mainz, Effect of Na presence during CuInSe $_2$ growth on stacking fault annihilation and electronic properties, Appl. Phys. Lett. 107 (2015) 152103. doi:10.1063/1.4933305.

[7] O. Lundberg, J. Lu, A. Rockett, M. Edoff, L. Stolt, Diffusion of indium

and gallium in Cu(In,Ga)Se2 thin film solar cells, J. Phys. Chem. Solids. 64 (2003) 1499–1504. doi:10.1016/S0022-3697(03)00127-6.

[8] A. Laemmle, R. Wuerz, M. Powalla, Efficiency enhancement of Cu(In,Ga)Se $_2$ thin-film solar cells by a post-deposition treatment with potassium fluoride, Phys. Status Solidi - Rapid Res. Lett. 7 (2013) 631–634. doi:10.1002/pssr.201307238.

[9] N. Nicoara, T. Lepetit, L. Arzel, S. Harel, N. Barreau, S. Sadewasser, Effect of the KF post-deposition treatment on grain boundary properties in Cu(In, Ga)Se2 thin films, Sci. Rep. 7 (2017) 41361. doi:10.1038/srep41361.

[10] F. Pianezzi, P. Reinhard, A. Chirilă, B. Bissig, S. Nishiwaki, S. Buecheler, A.N. Tiwari, Unveiling the effects of post-deposition treatment with different alkaline elements on the electronic properties of CIGS thin film solar cells, Phys. Chem. Chem. Phys. 16 (2014) 8843. doi:10.1039/c4cp00614c.

[11] A. Chirilă, P. Reinhard, F. Pianezzi, P. Bloesch, A.R. Uhl, C. Fella, L. Kranz, D. Keller, C. Gretener, H. Hagendorfer, D. Jaeger, R. Erni, S. Nishiwaki, S. Buecheler, A.N. Tiwari, Potassium-induced surface modification of Cu(In,Ga)Se2 thin films for high-efficiency solar cells, Nat. Mater. 12 (2013) 1107–1111. doi:10.1038/nmat3789.

[12] P.M.P. Salomé, V. Fjällström, P. Szaniawski, J.P. Leitão, A. Hultqvist, P.A. Fernandes, J.P. Teixeira, B.P. Falcão, U. Zimmermann, A.F. da Cunha, M. Edoff, A comparison between thin film solar cells made from co-evaporated CuIn $_{1-x}$ Ga $_x$ Se $_2$ using a one-stage process versus a three-stage process, Prog. Photovoltaics Res. Appl. 23 (2015) 470–478. doi:10.1002/pip.2453.

[13] F. Werner, M.H. Wolter, S. Siebentritt, G. Sozzi, S. Di Napoli, R. Menozzi, P. Jackson, W. Witte, R. Carron, E. Avancini, T.P. Weiss, S. Buecheler, Alkali treatments of Cu(In,Ga)Se $_2$ thin-film absorbers and

their impact on transport barriers, Prog. Photovoltaics Res. Appl. 26 (2018) 911–923. doi:10.1002/pip.3032.

[14] T.P. Weiss, S. Nishiwaki, B. Bissig, S. Buecheler, A.N. Tiwari, Voltage dependent admittance spectroscopy for the detection of near interface defect states for thin film solar cells, Phys. Chem. Chem. Phys. 19 (2017) 30410–30417. doi:10.1039/C7CP05236G.

[15] S. Siebentritt, Shallow Defects in the Wide Gap Chalcopyrite CuGaSe2, in: Wide-Gap Chalcopyrites, Springer-Verlag, Berlin/Heidelberg, 2006: pp. 113–156. doi:10.1007/3-540-31293-5_7.

[16] R. Mainz, E. Simsek Sanli, H. Stange, D. Azulay, S. Brunken, D. Greiner, S. Hajaj, M.D. Heinemann, C.A. Kaufmann, M. Klaus, Q.M. Ramasse, H. Rodriguez-Alvarez, A. Weber, I. Balberg, O. Millo, P.A. van Aken, D. Abou-Ras, Annihilation of structural defects in chalcogenide absorber films for high-efficiency solar cells, Energy Environ. Sci. 9 (2016) 1818–1827. doi:10.1039/C6EE00402D.